

NEW SURFACE REFLECTANCE MODEL WITH THE COMBINATION OF TWO CUBIC FUNCTIONS USAGE

Oleksandr Romanyuk¹, Yevhen Zavalniuk¹, Sergii Pavlov¹, Roman Chekhmestruk², Zlata Bondarenko¹, Tetiana Koval³, Aliya Kalizhanova⁴, Aigul Iskakova⁵

¹Vinnitsia National Technical University, Vinnitsia, Ukraine, ²3D GENERATION UA, Vinnitsia, Ukraine, ³Mykhailo Kotsiubynskyi State Pedagogical University, Vinnitsia Ukraine, ⁴University of Power Engineering and Telecommunications; Institute of Information and Computational Technologies MES CS RK, Almaty, Kazakhstan, ⁵Kazakh National Research Technical University named after K. I. Satpayev, Almaty, Kazakhstan

Abstract. In the article the model of light reflection based on the combination of two cubic bidirectional reflectance distribution functions is developed. The main components of color and the main requirements for reproducing the object's glares are analyzed. The usage characteristics of Cook-Torrance, Bagher, Oren-Nayar, coupled Shirley reflection models are described. The advantages and disadvantages of the highly productive Blinn-Phong model are considered. The necessity of approximating the Blinn-Phong model by a function of low degree is justified. The characteristics of the cubic polynomial approximation of the Blinn-Phong model are determined. It was established that the main drawback of this approximation is a significant deviation of the function from the reference function in the glare's attenuation zone. The combined function that combines two cubic functions is proposed. The first cubic function reproduces the glare's epicenter, and the second replaces the specified function in the attenuation zone. A system of equations for calculating the coefficients of the second function was created. The formula for the connection point of two cubic functions is obtained. A graph of the developed combined model based on cubic functions is obtained. For the combined and original cubic functions a comparison of the maximum relative errors in the glare's epicenter zone, the maximum absolute errors, and the relative errors at the inflection point was made. A three-dimensional plot of the absolute error of the combined cubic model from the Blinn-Phong model depending on the shininess and the angle value is built. Visualization results based on the combined and the original cubic functions are compared. It is confirmed that the proposed reflection model increases the realism of glare formation in the attenuation zone. The resulting combined reflection model provides a highly accurate approximation of the Blinn-Phong model and is highly efficient because the third power function is used.

Keywords: bidirectional reflectance distribution function, cubic function, reflectance model, shading, combined function

NOWY MODEL ODBICIA ŚWIATŁA OD POWIERZCHNI WYKORZYSTUJĄCY KOMBINACJĘ DWÓCH FUNKCJI SZEŚCIENNYCH

Streszczenie. W artykule opracowano model odbicia światła oparty na kombinacji dwóch sześciennych dwukierunkowych funkcji rozkładu odbicia. Przeanalizowano główne składniki koloru i główne wymagania dotyczące odtwarzania odbłasków obiektu. Opisano charakterystykę użytkowania modeli odbicia Coocka-Torrance'a, Baghera, Orena-Nayara i Shirleya. Rozważono zalety i wady wysoce wydajnego modelu Blinn-Phong. Uzasadniono konieczność aproksymacji modelu Blinna-Phonga funkcją niskiego stopnia. Określono charakterystykę wielomianu sześciennego aproksymującego model Blinna-Phonga. Ustalono, że główną wadą tej aproksymacji jest znaczne odchylenie funkcji od funkcji odniesienia w strefie tłumienia oślnienia. Zaproponowano funkcję kombinowaną, która łączy dwie funkcje sześcienne. Pierwsza funkcja sześcienna odtwarza epicentrum oślnienia, a druga zastępuje określoną funkcję w strefie tłumienia. Stworzono układ równań do obliczania współczynników drugiej funkcji. Uzyskano wzór na punkt połączenia dwóch funkcji sześciennych. Uzyskano wykres opracowanego połączonego modelu opartego na funkcjach sześciennych. Dla połączonych i oryginalnych funkcji sześciennych dokonano porównania maksymalnych błędów względnych w strefie epicentrum oślnienia, maksymalnych błędów bezwzględnych i błędów względnych w punkcie przegięcia. Zbudowano trójwymiarowy wykres błędu bezwzględnego połączonego modelu sześciennego z modelu Blinna-Phonga w zależności od połysku i wartości kąta. Porównano wyniki wizualizacji oparte na połączonych i oryginalnych funkcjach sześciennych. Potwierdzono, że proponowany model odbicia zwiększa realizm powstawania odbłasków w strefie tłumienia. Wynikowy połączony model odbicia zapewnia bardzo dokładne przybliżenie modelu Blinna-Phonga i jest bardzo wydajny, ponieważ używana jest funkcja trzeciej potęgi.

Słowa kluczowe: dwukierunkowa funkcja rozkładu współczynnika odbicia, funkcja sześcienna, model współczynnika odbicia, cieniowanie, funkcja łączona

Introduction

Modern three-dimensional rendering systems must meet the requirements of high performance and high realism. In order to create realistic three-dimensional graphic images, it is necessary to take into account the features of light reflection from the objects' surfaces in the scene. For this, during the surface shading, the three components of color [10, 11] are taken into account - ambient, diffuse and specular. The process of finding the specular [17] component of color is the most time-consuming, as it involves the calculation of normalized vectors to the observer, to the light source, and the normal vector. After this the lighting model, which has a high degree, is calculated and the color intensities for the RGB components are determined.

The main requirements for the reproduction of glares on the surfaces of objects are highly productive performance, highly accurate reproduction of the epicenter zone, and realistic reproduction of the attenuation zone. The existing models of light reflection do not comprehensively meet all the three requirements. Therefore, it is necessary to develop effective new models of the surface reflectivity, which provide a more highly productive implementation of rendering [15, 18].

1. Literature overview

The characteristics of the spatial reflection of light [14] from the surface are presented using the bidirectional reflectance distribution function (BRDF) [13]. BRDF is a function of the zenith and azimuthal angles (respectively, θ , ϕ) of the vectors to the light source and the observer (Fig. 1). In order to calculate the BRDF, the radiance of reflected light and the irradiance of light that fell on the surface are determined.

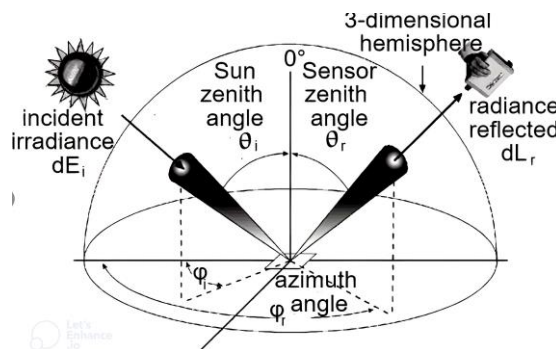


Fig. 1. Data for BRDF calculation [9]

BRDF is calculated according to the formula [14]

$$\frac{dL_r(\theta_i, \phi_i, \theta_r, \phi_r, \lambda)}{dE(\theta_i, \phi_i)} \quad (1)$$

where L_r – the radiance of light, E – irradiance of light, λ – the wave length.

BRDFs are divided into physically accurate and empirical.

Physically accurate [6, 7] BRDFs are more accurate and usually take into account the division of the object's surface into facets. The physically accurate BRDFs include the Cook-Torrance [5, 6], Bagher [1], Oren-Nayyar [6, 12], coupled Shirley [3, 6] models [1, 16, 19].

In the Cook-Torrance model [6] it is taken into account that the reflectivity of the surface is affected by micro-facets [6], oriented along the vector $\vec{H} = (\vec{L} + \vec{V}) / |\vec{L} + \vec{V}|$, where \vec{L} and \vec{V} , respectively, are the vectors to the light source and the observer. The model includes a diffuse component, represented by Lambertian reflection, and a specular component. During the calculation of the specular component, the Fresnel factor F , the geometric shading factor G , and the distribution of micro-facets D are used. The specular component of this BRDF is calculated according to the formula [5, 6]

$$\frac{FDG}{\pi(\vec{N} \cdot \vec{L})(\vec{N} \cdot \vec{V})} \quad (2)$$

Bagher model [1] is an improvement of the Cook-Torrance model and lies in the usage of the SGD distribution (shifted gamma distribution) of micro-facets. Due to the usage of this distribution, compliance of the model with the measured characteristics of the most materials is ensured. SGD distribution is calculated according to the formula

$$\frac{\chi[0; \pi/2](\theta_m)}{\pi \cos(\theta_m)^4} \left(\frac{\alpha^{p-1}}{\Gamma(1-p, \alpha)} \right) \left(\frac{e^{-\alpha^2 + \tan(\theta_m)^2}}{\alpha} \right) \left(\frac{1}{(\alpha^2 + \tan(\theta_m)^2)^p} \right) \quad (3)$$

where θ_m – the angle between surface and micro-facet normals, $\chi[0; \pi/2] = 1$ if $\theta_m < \pi/2$, $\chi[0; \pi/2] = 0$ if $\theta_m \geq \pi/2$, Γ – incomplete gamma-function, p – the parameter of model, α – the roughness.

The Oren-Nayard model [6, 12] is an improvement of the Lambert model. It is calculated according to the formula

$$\begin{aligned} & \frac{\rho}{\pi} \left((1 - 0.5 \frac{\alpha_m^2}{\alpha_m^2 + 0.33}) + \right. \\ & + 0.45 \frac{\alpha_m^2}{\alpha_m^2 + 0.09} \max(0, \cos(\phi_{w_i} - \phi_{w_o})) \cdot \\ & \cdot \sin(\max(\theta_{w_o}, \theta_{w_i})) \tan(\min(\theta_{w_o}, \theta_{w_i})) \left. \right) \end{aligned} \quad (4)$$

where α_m^2 – object's surface roughness, w_i, w_o – the light source and observer vectors respectively.

The coupled Shirley BRDF [3, 6] connects the diffuse and specular color components. The latter component is applied to polished surfaces of dielectrics. The model is energetically plausible. It is calculated according to the formula

$$\begin{aligned} & [R_0 + (1 - \cos(\omega_o))^5 (1 - R_0)] f_{r,s}(w_o, w_i) + \\ & + k R_m [1 - (1 - \cos(\omega_o))^5] [1 - (1 - \cos(\omega_i))^5] \end{aligned} \quad (5)$$

where k – normalization constant, R_m – the reflectance of matte component, R_0 – parameter [0.03, 0.06].

The disadvantage of this group of BRDFs is significant computational costs, therefore, physically accurate BRDFs are rarely used in highly productive graphic systems.

Among the empirical models, characterized by high productivity and approximation accuracy of light reflection, the Blinn and Phong BRDFs are the most often used.

For the calculation of Phong BRDF [4], a vector to the observer and a specular reflection vector \vec{R} are used. Phong BRDF is calculated by the formula $\cos(\psi)^n$, where ψ – is the angle between \vec{V} and \vec{R} , n is the shininess coefficient of the surface.

One of the disadvantages of the model is the possibility of a larger ψ value than 90° , which can lead to the appearance of image artifacts.

In the Blinn model [2] the angle γ between the vectors \vec{N} and \vec{H} , which does not exceed 90° , is used instead of ψ . \vec{N} is a normal to the surface.

When the n values are big the Blinn and Phong BRDFs do not meet the requirements of highly productive graphics systems. Therefore, for the Blinn-Phong model the approximating BRDFs are used.

For the Blinn-Fong model approximation by a cubic function [8] the calculated coefficients A, B, C , which depend on the shininess coefficient, are used.

The cubic model of light reflection is calculated according to the formula [8]

$$A \cos(\gamma)^3 + B \cos(\gamma)^2 + C \cos(\gamma) \quad (6)$$

The values of the Q, G points of the ordinate axis are used to calculate the coefficients of the model. The point Q is usually located near the level of the inflection point of the function. The point G is located near the zero of the ordinate axis and is used to control the size of the glare's attenuation zone.

The coefficient A is calculated according to the formula

$$\frac{LR(R-L) + GR(1-R) + LQ(L-1)}{L^3(R-R^2) + L^2(R^3-R) - LR^2(R-1)} \quad (7)$$

where $R = \cos(t)$, $L = \cos(u)$, t, u – abscissa axis points that correspond to ordinate axis points Q, G .

The coefficient B is calculated according to the formula

$$\frac{GR(R^2-1) + LR(L^2-R^2) + QL(1-L^2)}{L^3(R-R^2) + L^2(R^3-R) - LR^2(R-1)} \quad (8)$$

The coefficient C is calculated according to the formula

$$\frac{GR(R-R^2) + L^2Q(L-1) + LR(LR^2-L^2R)}{L^3(R-R^2) + L^2(R^3-R) - LR^2(R-1)} \quad (9)$$

For this function it was established that the optimal Q, G values are 0.5, 1/18 [8].

Fig. 2 shows the plot of A, B, C coefficients values when $Q = 0.5, G = 1/18$ and $n \in [4, 256]$.

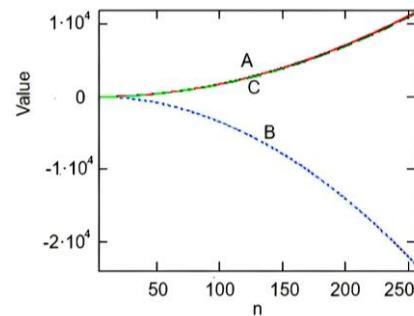


Fig. 2. The plot of A, B, C coefficients values

As shown in the figure, the coefficients A and C have similar values.

Let us denote the considered cubic function F_{KUB1} , which is an approximation of the Blinn-Fong BRDF (F_B). Fig. 3 shows the graphs of F_{KUB1} and F_B when $n = 50$.

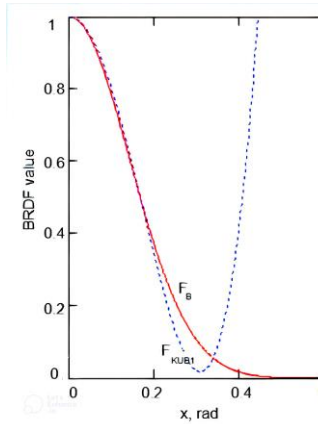


Fig. 3. The plots of F_B , F_{KUB1} when $n = 50$

The disadvantage of F_{KUB1} is an insufficiently accurate approximation of F_B in the attenuation zone, which leads to an unnatural reproduction of glare's attenuation. Therefore, the F_{KUB1} improvement is necessary to ensure a more accurate F_B approximation.

2. Aim of the research

The aim of the paper is to develop the new lighting model through using the combination of two cubic BRDFs in order to provide the more accurate glare reproduction in the attenuation zone.

3. The development of combined BRDF based on polynomial cubic functions

To ensure a highly accurate F_B approximation, we combine F_{KUB1} with another cubic function, which will allow us to more accurately reproduce the attenuation zone of the glare.

For the connection of F_{KUB1} with the new cubic function F_{KUB2} , we will choose the level of the ordinate axis 0.5, below which the values of F_{KUB1} and F_B are noticeably different.

Let's determine the coefficient formulas for F_{KUB2} using a system of equations. The first equation corresponds to the level $\cos(E)^n = 0.5$, the second equation corresponds to the level $\cos(t)^n = Q$, the third to the level $\cos(u)^n = G$, the fourth to the level $\cos(\pi/2)^n = 0$. The system of equations is defined as

$$\begin{cases} A2 \cdot \cos(E)^3 + B2 \cdot \cos(E)^2 + C2 \cdot \cos(E) + D2 = 0.5 \\ A2 \cdot \cos(t)^3 + B2 \cdot \cos(t)^2 + C2 \cdot \cos(t) + D2 = Q \\ A2 \cdot \cos(u)^3 + B2 \cdot \cos(u)^2 + C2 \cdot \cos(u) + D2 = G \\ D2 = 0 \end{cases} \quad (10)$$

where $E = a \cos(e^{-0.693/n})$.

From the system we find that the coefficient $A2$ is calculated according to the formula

$$0.5 \frac{LR(R-L) + GR(2E^2 - R2E) + LQ(L2E - 2E^2)}{L^3(RE^2 - R^2E) + L^2(R^3E - RE^3) - LR^2(RE^2 - E^3)} \quad (11)$$

where $E = e^{-0.693/n}$.

$B2$ is calculated according to the formula

$$0.5 \frac{GR(R^22E - 2E^3) + LR(L^2 - R^2) + QL(2E^3 - L^22E)}{L^3(RE^2 - R^2E) + L^2(R^3E - RE^3) - LR^2(RE^2 - E^3)} \quad (12)$$

$C2$ is calculated according to the formula

$$0.5 \frac{GR(R2E^3 - R^22E^2) + L^2Q(L2E^2 - 2E^3) + LR(LR^2 - L^2R)}{L^3(RE^2 - R^2E) + L^2(R^3E - RE^3) - LR^2(RE^2 - E^3)} \quad (13)$$

Fig. 4 shows the plots of F_{KUB2} , $A2$, $B2$, $C2$ coefficients values when $Q = 0.1$, $G = 1/40$ and $n \in [4, 256]$.

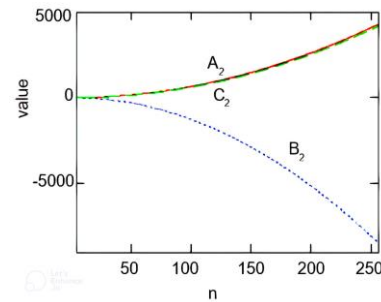


Fig. 4. The plots of $A2$, $B2$, $C2$ coefficients values

It is advisable to store the calculated F_{KUB1} and F_{KUB2} coefficients in a block of permanent memory, since they are the same for all cases of calculation of BRDF.

Fig. 5 shows the plots of F_{KUB2} , F_{KUB1} and F_B when $n = 50$. The selected values for Q, G, F_{KUB2} are 0.1, 1/40.

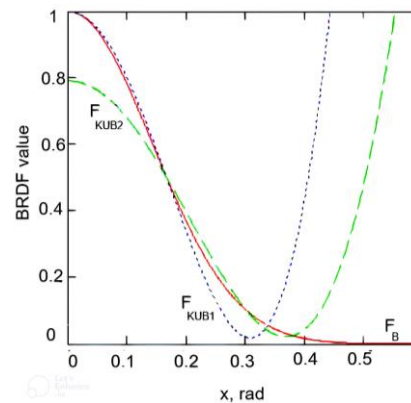


Fig. 5. The plots of F_B , F_{KUB2} , F_{KUB1} when $n = 50$

As can be seen from the figure, the combination of F_{KUB2} , F_{KUB1} at the point 0.5 provides a highly accurate approximation of F_B in the epicenter and attenuation zones.

Let's find the abscissa of the connection point of F_{KUB1} and F_{KUB2} . We equate the calculation formulas of F_{KUB1} and F_{KUB2}

$$\begin{aligned} A \cdot \cos(x)^3 + B \cdot \cos(x)^2 + C \cdot \cos(x) &= \\ = A2 \cdot \cos(x)^3 + B2 \cdot \cos(x)^2 + C2 \cdot \cos(x) & \quad (14) \end{aligned}$$

From the equation, we find the formula for the point of connection of F_{KUB1} and F_{KUB2} $connect(n)$

$$connect(n) = a \cos(e^{-0.693/n}) \quad (15)$$

With the usage of MS Excel the simplified calculation expressions of $connect(n)$ ($connect_appr(n)$) depending on n were obtained

$$\begin{cases} (\frac{1}{2^9} - \frac{1}{2^{12}})n^2 - (\frac{1}{2^5} + \frac{1}{2^6} + \frac{1}{2^7})n + (\frac{1}{2^1} + \frac{1}{2^2}), n \geq 4 \wedge n \leq 16 \\ (\frac{1}{2^{15}} + \frac{1}{2^{16}} + \frac{1}{2^{18}})n^2 - (\frac{1}{2^7} - \frac{1}{2^{10}})n + (\frac{1}{2^2} + \frac{1}{2^3}), n > 16 \wedge n \leq 70 \\ (\frac{1}{2^{19}} - \frac{1}{2^{22}})n^2 - (\frac{1}{2^{10}} - \frac{1}{2^{13}})n + (\frac{1}{2^3} + \frac{1}{2^4}), n > 70 \wedge n \leq 256. \end{cases} \quad (16)$$

Fig. 6 shows the plots of $connect_appr(n)$ and $connect(n)$ depending on the values $n \in [4,256]$.

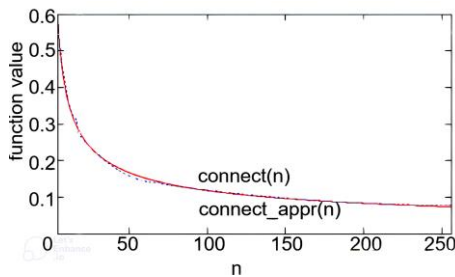


Fig. 6. The plots of original and approximated formulas of calculation of the cubic functions connection point

Therefore, a high-precision approximation of the original formula of the cubic functions connection point is ensured.

To ensure the smoothness of the connection of two cubic functions, a 0.5 level was chosen. Finding the derivatives of functions F_{KUB1} and F_{KUB2} is not necessary, since the values of functions are similar at a sufficiently large interval near $connect(n)$ (Fig. 7 shows the absolute deviation between F_{KUB1} and F_{KUB2} for $n \in [50,200]$).

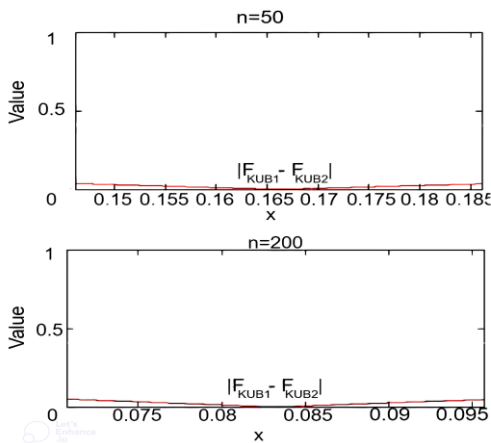


Fig. 7. The plots of absolute deviation between F_{KUB1} and F_{KUB2} near their connection point

We denote the developed combined function as F_{KUB3} .

Fig. 8 shows the graphs of F_{KUB1} , F_{KUB3} and F_B when $n = 50$.

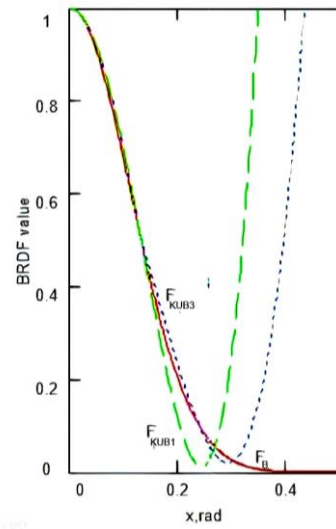


Fig. 8. The plots of F_{KUB1} , F_{KUB3} and F_B when $n = 50$

Through using the combination of two cubic functions in F_{KUB3} , an increase in the accuracy of the approximation of the glare's attenuation zone has been achieved.

Since the F_{KUB1} and F_{KUB3} coincide in the zone of the glare's epicenter, their maximum relative errors δ of F_B approximation in the epicenter are equal (2.95%, Fig. 9).

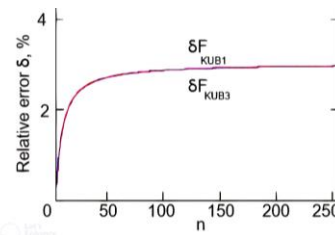


Fig. 9. The plots of maximum relative errors of F_{KUB1} and F_{KUB3} in glare's epicenter

Fig. 10 shows the plots of the relative errors of F_{KUB1} and F_{KUB3} from F_B at the inflection point that is separating the epicenter and attenuation zones. The plot is built relative to the values of $n \in [4,256]$.

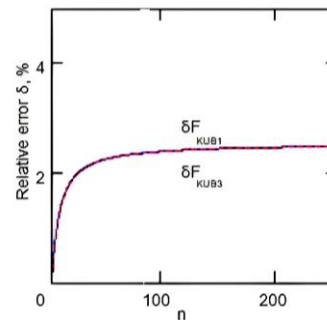


Fig. 10. The plots of relative errors of F_{KUB1} and F_{KUB3} at the F_B inflection point

The maximum relative error of F_{KUB1} and F_{KUB3} from F_B in its inflection point is 2.5%.

Fig. 11 shows the plots of maximum absolute errors Δ of F_{KUB1} and F_{KUB3} from F_B depending on $n \in [4,256]$.

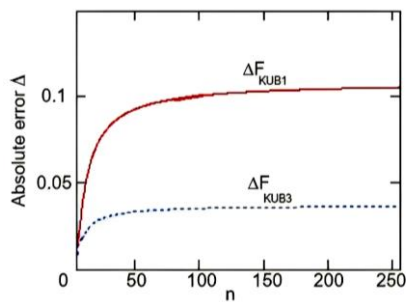


Fig. 11. The plots of absolute errors of F_{KUB1} and F_{KUB3} from F_B

It is worth noting that the maximum absolute error of F_{KUB1} from the known function is 0.11, it's unacceptable. Maximum absolute error of F_{KUB3} from F_B is 0.035. Therefore, F_{KUB3} in comparison with F_{KUB1} provides more accurate F_B approximation.

Fig. 12 shows the plot of absolute errors between F_{KUB3} and F_B depending on $n \in [4, 256]$ and $x \in [0; \pi/2]$ values.

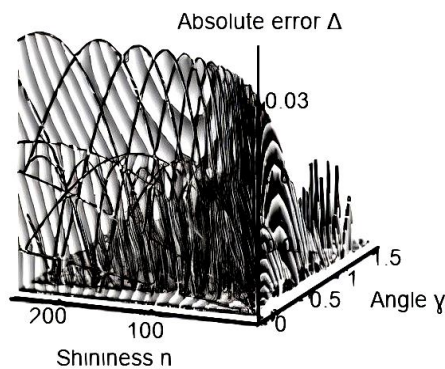


Fig. 12. The plot of absolute errors between F_{KUB3} and F_B depending on angle value and shininess

Based on F_{KUB1} and F_{KUB3} the test figure "Teapot" was visualized in BRDF Explorer. The visualization result is given in Fig. 13.

References

- [1] Avrunin O. G., Tymkovych M. Y., Abdelhamid I. Y., Shushliapina N. O., Nosova Y. V., Semenets V. V.: Features of image segmentation of the upper respiratory tract for planning of rhinosurgical surgery. IEEE 39th International Conference on Electronics and Nanotechnology, ELNANO 2019, 485–488.
- [2] Bagher M.: Accurate fitting of measured reflectances using a Shifted Gamma micro-facet distribution. Computer Graphics Forum 31(4), 2012, 1509–1518.
- [3] Han Yu. et al.: Learning a 3D Morphable Face Reflectance Model from Low-cost Data. arXiv: 2303.11686, 2023.
- [4] Jakob W. et al.: A Comprehensive Framework for Rendering Layered Materials. ACM Transactions on Graphics 33(4), 2014, 1–14.
- [5] Kurt M.: Real-Time Shading with Phong BRDF Model. DEUFMD 21(63), 2019, 859–867.
- [6] Liu H. et al.: Development of a Face Recognition System and Its Intelligent Lighting Compensation Method for Dark-Field Application. IEEE Transactions on Instrumentation and Measurement 70, 2021, 1–16.
- [7] Montes R., Urena C.: An Overview of BRDF Models. University of Granada, 2012.
- [8] Romanyuk A. The Bidirectional Reflectance Distributive Function Classification Scientific Papers of Donetsk National Technical University 9, 2008, 145–151.
- [9] Romanyuk O., Chorny A.: Vysokoproduktyvni metody ta zasoby zafarbovuvannya tryvymirnykh hrafichnykh ob'ektiv. UNIVERSUM-Vinnitsya, Vinnitsya, 2006.

Fig. 13 shows that F_{KUB3} provides a more realistic formation of the glare's attenuation zone.

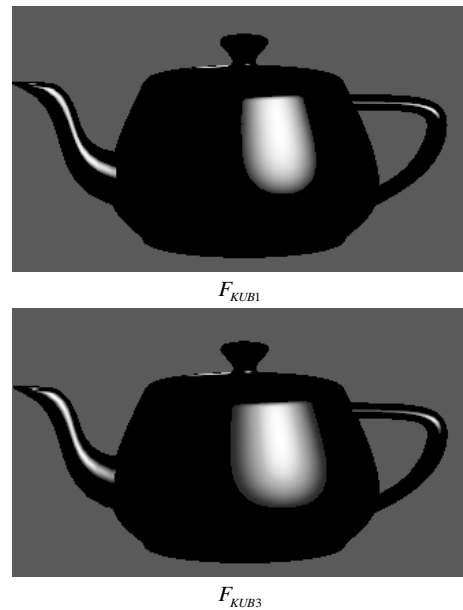


Fig. 13. The visualized teapots based on F_{KUB1} and F_{KUB3}

4. Conclusions

The article proposes a model of surface reflectance based on the combination of two cubic functions. The developed model is an improvement of a separate cubic model [8] and provides an increase in the accuracy of the approximation of the widely used Blinn-Fong model. The model combines the original cubic function and the new cubic function with calculated formulas of coefficients.

The developed combined model was compared to the original cubic model. It is shown that the developed model provides highly accurate reproduction of both the glare's epicenter and its attenuation.

The developed model is intended for use in highly realistic graphic systems.

- [10] Romanyuk O.: Komp'yuterna hrafika: Navchal'nyy posibnyk. VDTU, Vinnytsya 1999.
- [11] Romanyuk O. et al.: The Concept and Means of Adaptive Shading. 12th International Conference on Advanced Computer Information Technologies (ACT), Ruzomberok, 2022, 33–38.
- [12] Romanyuk S., Pavlov S., Wójcik W. et al.: Using lights in a volume-oriented rendering. Proc. SPIE 10445, 2017, 104450U.
- [13] Schill S. et al.: Temporal Modeling of Bidirectional Reflection Distribution Function (BRDF) in Coastal Vegetation. GIScience & Remote Sensing 41(2), 2004, 116–134.
- [14] Tan P.: Phong Reflectance Model. Computer Vision, 2020, 1–3.
- [15] Thiele S. et al.: A Novel and Open-Source Illumination Correction for Hyperspectral Digital Outcrop Models. IEEE Transactions on Geoscience and Remote Sensing 60, 2022, 1–12.
- [16] Wójcik W., Pavlov S., Kalimoldayev M.: Information Technology in Medical Diagnostics II. Taylor & Francis Group, CRC Press, Balkema book, London 2019.
- [17] Wójcik W., Smolarz A.: Information Technology in Medical Diagnostics. CRC Press, 2017.
- [18] Zavalniuk Ye. K. et al.: The development of the modified schlick model for the specular color component calculation. Information technology and computer engineering 55(3), 2022, 4–12.
- [19] Zou Ya. et al.: Developmental Trends in the Application and Measurement of the Bidirectional Reflection Distribution Function. Sensors 22 (5), 2022, 1739–1763.

Prof. Oleksandr N. Romanyuk

e-mail: rom8591@gmail.com

Doctor of Technical Sciences, professor, Head of Department of Software Engineering of Vinnytsia National Technical University.
Research field: formation and processing of graphic images.

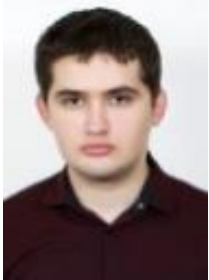


<http://orcid.org/0000-0002-2245-3364>

M.Sc. Yevhen K. Zavalniuk

e-mail: qq9272627@gmail.com

Ph.D. student, Department of Software Engineering of Vinnytsia National Technical University.
Research interests include formation and processing of graphic images.



<http://orcid.org/0009-0005-1202-4653>

Prof. Sergii Pavlov

e-mail: psv@vntu.edu.ua

Academician of International Applied Radioelectronic Science Academy, Professor of Biomedical Engineering and Optic-Electronic Systems Department, Vinnytsia National Technical University. Scientific direction – biomedical information optoelectronic and laser technologies for diagnostics and physiotherapy influence. Deals with issues of improving the distribution of optical radiation theory in biological objects, particularly through the use of electro-optical systems, and the development of intelligent biomedical optoelectronic diagnostic systems and standardized methods for reliably determining the main hemodynamic cardiovascular system of comprehensive into account scattering effects.



<http://orcid.org/0000-0002-0051-5560>

PhD Roman Y. Chekhmestruk

e-mail: Rc.ua@3dgeneration.com

Candidate of Technical Sciences. Technical Director 3D GENERATION UA, research field: formation and processing of graphic images.



<http://orcid.org/0000-0002-5362-8796>

Ph.D. Zlata Bondarenko

e-mail: bondarenko@vntu.edu.ua

Associate professor of the Department of Higher Mathematics, Vinnytsia National Technical University.
Scientific direction – innovative technologies for training future specialists in technical specialties.



<http://orcid.org/0000-0003-3339-0570>

Ph.D. Tetiana Koval

e-mail: tanyabyzja@ukr.net

Candidate of Pedagogic Sciences, associate professor at the Department of Artistic Disciplines, Preschool and Elementary Education, Vinnytsia Mykhailo Kotsiubynskyi State Pedagogical University, Vinnytsia Ukraine
Research field: information technologies in pedagogic



<http://orcid.org/0000-0002-3190-1181>

Ph.D. Aliya Kalizhanova

e-mail: kalizhanova_aliya@mail.ru

Candidate of physical and mathematical sciences, professor at University of Power Engineering and Telecommunications, the chief researcher of the Institute of Information and Computational Technologies of the Ministry of Education and Science CS of the Republic of Kazakhstan. Scientific interests of the leader: mathematical modeling of systems, models of transport systems network analysis, optimization methods, technologies for developing sensor systems for signals receive - transmit, mathematical modeling of Bragg fiber gratings.



<http://orcid.org/0000-0002-5979-9756>

M.Sc. Eng. Aigul Iskakova

e-mail: Iskakova1979@mail.ru

Lecturer of the Kazakh National Research Technical University named after K. I. Satpayev.
Total number of scientific and methodological developments and articles – more than 45.



<http://orcid.org/0000-0001-8043-819X>